Nanoscale

Sulfur-Treated TiO2 Shows Improved Alcohol Dehydration Activity and Selectivity

Journal:	*Nanoscale*
Manuscript ID	NR-ART-09-2021-006029.R1
Article Type:	Paper
Date Submitted by the Author:	03-Jan-2022
Complete List of Authors:	Riscoe, Andrew; Stanford University, Chemical Engineering Oh, Jinwon; Stanford University, Materials Science and Engineering Cargnello, Matteo; Stanford University, Chemical Engineering

Sulfur-Treated TiO_2 Shows Improved Alcohol Dehydration Activity and Selectivity

Andrew Riscoe,[1] Jinwon Oh,[2] Matteo Cargnello[1]

[1]*Department of Chemical Engineering, Stanford University, Stanford, CA 94305, USA*

[2]*Department of Materials Science and Engineering, Stanford University, Stanford, CA 94305, USA*

Abstract

The dehydration of alcohols is an important class of reactions for the development of fossil-free fuel and chemical industries. Acid catalysts are well known to enhance reactivity of alcohols following two main pathways of either dehydration to olefins or dehydrogenation to ketones/aldehydes. TiO_2 surfaces have been well documented for primary and secondary alcohol dehydration with selectivity ranging from 1-100% towards dehydration products based on process conditions and catalyst structure. In this work we document the effects of various sulfur treatments of TiO_2 surfaces which induce higher activity and, more importantly, higher selectivity for alcohol dehydration than untreated surfaces. The increase in activity and >99% dehydration selectivity is coupled with demonstrated stability for several hours on stream at high conversion. Using temperature programmed reaction studies, XPS and FT-IR spectroscopy we identify Lewis acidic sites correlated with sulfate species on TiO_2 surfaces as active sites for the reaction.

Introduction

The dehydration of alcohols into olefins and other reduced carbonaceous species is of importance to the production or fuels and chemicals from non-fossil-based sources. Such carbon sources like biofeedstocks generally display a large oxygen content, which often takes the form of either single or polyhydroxylated carbons in addition to ether and ester linkages throughout a larger carbon framework. Dehydration of glucose, for instance, has been intensively studied[1,2] to produce hydroxymethylfurfural (HMF), which is considered an essential component to a fossil carbon-free future chemical industry.[3] Other poly-hydrated hydrocarbons have been studied where selective dehydration can be demonstrated with certain catalysts to yield more desired alcohol products.[4,5] Small alcohols, like ethanol and propanol are also dehydration targets as the corresponding olefin products, ethylene and propylene, are in high demand since both are precursors for chemical synthesis and monomers for plastic production.[6,7] These latter reactions are used as probe reactions to translate catalyst performance to other alcohol substrates.[8] For these alcohols, selectivity of dehydration rather than dehydrogenation to reactive aldehyde/ketone species is important for catalyst and downstream process stability[9].

Dehydration of alcohols has been demonstrated on metal oxide surfaces since the 1970s.[10–12] Since then, many hypotheses have been claimed to link the activity to mechanisms and active sites. Acids (both Lewis and Brønsted) are known to catalyze the dehydration of alcohols. For this reason, it has been proposed that the selectivity towards dehydration rather than dehydrogenation allows a convenient method of determination of acid/base character of a metal oxide surface.[11,13] However, recently it has been pointed out that the reducibility of the metal oxide surface compromises this direct link of surface acidity to its dehydration activity, making the selectivity to dehydration of probe alcohols a less straightforward metric.[14–16] Nevertheless, the connection between acid character and dehydration activity remains.

TiO_2 has been investigated for this reaction. It is moderately reducible[17] and has been the subject of many efforts to discern the mechanism that governs its performance, and a collection of results in using it for dehydration of both primary and secondary alcohols is reported in Table 1 and plotted in Figure 1. TiO_2 is known to possess catalytically active Lewis acid sites with both high and low acid strength.[18] Despite the extensive study on using TiO_2 for secondary alcohol dehydration, there are many conflicting reports of activity and selectivity (See Table 1). Reaction

conditions appear to determine the selectivity: for example, Barteau and coworkers report near complete selectivity to dehydrogenation of isopropanol on anatase TiO_2 in continuous reaction studies using a packed bed reactor;[16] other researchers found only traces of dehydrogenation products in a vacuum temperature programmed desorption study;[19] still other reports indicate results that are intermediate between these latter extremes.[14,20] These conflicting reports may be due to some differences in reaction conditions (space velocity, conversion, temperature etc.), yet based on these results it is not clear whether a TiO_2 catalysts would yield either dehydration or dehydrogenation products of a given alcohol in a reaction.

Table 1 Results from previous studies on alcohol dehydration with TiO_2 surfaces

Sample	Alcohol Studied	T (°C)	Feed Pressure (bar)	Conversion (%)	Dehydration Selectivity (%)	Ref.
Anatase TiO_2	2-propanol	200	0.012	6%	0.9%	16
Anatase TiO_2	2-propanol	325	0.016	4.12%	84%	16
Anatase TiO_2	1-butanol	250	0.0079	*	5%	20
Anatase TiO_2-PA	1-butanol	250	0.0079	*	65%	20
Rutile TiO_2	1-butanol	250	0.0079	*	39%	20
Rutile TiO_2 PA	1-butanol	250	0.0079	*	47%	20
Anatase TiO_2	2-butanol	210-290	00.0165	15%	8-85%	21
TiO_2 sol gel	ethanol	200-400	0.007434	13-45.00%	0-17%	22
TiO_2 (st)	ethanol	200-400	0.007434	21-56.3%	0-25.5%	22
P25 TiO_2	2-propanol	200	*	*	41%	14
Rutile TiO_2	2-propanol	202	*	*	0.6%	23
Anatase TiO_2	2-propanol	202	*	*	73%	23
P25 TiO_2	2-propanol	202	*	*	3.4%	23

* (not reported)

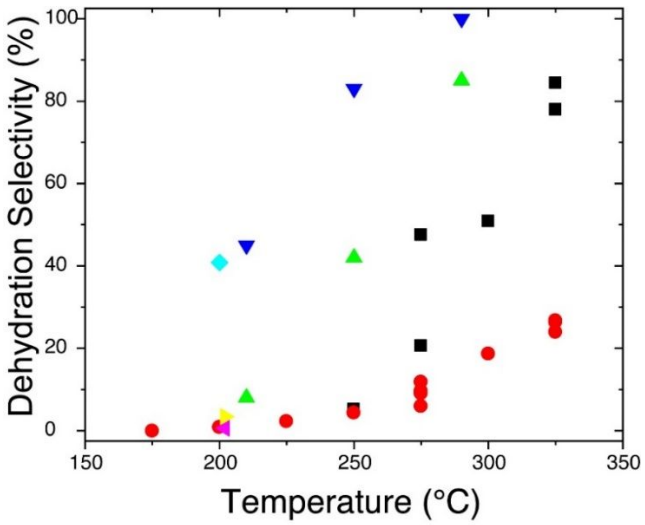

Figure 1. Dehydration selectivity of experimental studies of TiO_2 based catalysts in inert gases unless otherwise noted. Red circles = ref [16], (Anatase TiO_2 He + O_2 sweep gas), Black squares = ref [16] (anatase TiO_2), Green Triangles = ref [24] (anatase TiO_2) , Blue Triangles = ref [24] (anatase TiO_2 + H_3PO_4) , Teal Diamonds = [14] (commercial TiO_2 powder), Pink Triangle = ref [23] (Rutile TiO_2), Yellow Triangle = ref [23] (Commercial TiO_2)

Modification of catalytic surfaces to alter the electronic and geometric properties underlying any reaction mechanism is a promising approach for clarifying the role of active sites and improving catalytic performance. This approach has led to breakthroughs in understanding reaction mechanisms, as Nørskov and coworkers did to determine the role of step sites in nitrogen activation by blocking them with more inert atoms.[25] Likewise, it also provided advances in catalytic performance where, for instance, de Jong and coworkers demonstrated improvements in selectivity of Fisher-Tropsch catalysis with sulfur addition to catalytic surfaces.[26] Using this surface-modification approach in dehydration chemistry, by modifying TiO_2 surfaces with phosphonic acids Medlin and coworkers found that selectivity to dehydration was enhanced with the addition of highly active Brønsted acid sites balancing the decrease in the number of active sites after phosphonic acid treatment.[21] These examples highlight how surface modification can enhance reactivity and selectivity while also providing important clues to understand mechanisms of catalytic action.

In this study, we describe how the surface treatment of commercial TiO_2 powder with dimethylsulfoxide (DMSO) and other sulfur-containing species yields a more active and selective TiO_2 surface for alcohol dehydration. Low temperature (170 °C) turnover frequencies are increased by 50 times while selectivity is increased from roughly 50% selectivity for bare TiO_2 to 99% with DMSO-treated TiO_2 catalysts. Similarly, for ethanol dehydration, we observe a decrease in light-off temperature by nearly 100 °C coupled with maintaining >90% dehydration selectivity for sulfur-containing TiO_2 catalysts. The modified catalytic surfaces are stable, with catalysts performing similarly through five thermal cycles and 6 hours on stream. Further, we find that DMSO treatment improves TiO_2 catalysts activity for isopropanol dehydration to a higher degree than H_2SO_4 treatment. Using propylamine TPD, XPS, FT-IR and model catalysts tests, we propose that the high activity and selectivity are due to active sulfate species decorating the TiO_2 surface acting in concert with reduced poisoning of innate strongly Lewis acid sites on TiO_2 with DMSO treatment.

Experimental Section/Methods

Preparation of DMSO-Treated TiO_2. P25 TiO_2 (Acros) was calcined in air at 500 °C for 5 hours with 10 °C min^{-1} heating and cooling rates. Commercial reference TiO_2 was calcined in the same conditions. 1.5 g of calcined material was then added to a three-neck flask containing 58 mL of DMSO (Fisher, 99.7%). The resulting suspension was stirred under vacuum (<1 torr) for 5 minutes before switching to flowing N_2 and heating to 160 °C while stirring under reflux for 72 hours. The solid material was collected by centrifugation and washed with 60 mL acetone three times with centrifugation for 3 minutes at 8000 rpm to recover the solid after each round. After removing acetone under flowing air at room temperature, the solids were placed under reduced pressure (<200 torr) at 80 °C for 15 hours. The resultant solid was obtained with 93% yield as an off-white powder.

Preparation of H_2SO_4 Treated TiO_2. H_2SO_4 Treated TiO_2 was prepared from a modified synthesis based on published procedures[27] which used Calcined P-25 TiO_2. The particular ratio of H_2SO_4 to TiO_2 was chosen to match sulfur content from the DMSO-treated TiO_2 as determined by XPS. In this synthesis, 2.7 g of calcined P25 TiO_2 was added to 100 mL of 2-propanol (Sigma 99.5%), and to this suspension 2.08 mL of 1 M H_2SO_4 (aq) (prepared from neat H_2SO_4, Sigma 96.3%) were added under vigorous stirring. The suspension was stirred for 4 hours at 25 °C. After stirring, the solid was filtered and washed with 100 mL of isopropanol three times using centrifugation for 3 minutes at 8000 rpm to separate solids from solvent. After washing, the solid was dried for 12 hours under flowing air. Equal sulfur loading compared to DMSO-treated TiO_2 was verified with XPS Ti:S peak area measurements.

Structural characterization. A Nicolet is-50 with ATR attachment was used to collect FT-IR spectra. Spectra were collected with 1 cm^{-1} resolution with the average of 32 scans presented to improve the signal-to-noise ratio.

XPS spectra of materials were collected using a PHI VersaProbe III Scanning XPS Microprobe equipped with a hemispherical electron analyzer, Al (Kα, 1486.3 eV) source, aluminum holder and with argon ion gun and electron flood gun for charge neutralization. Materials were mixed with

mortar and pestle grinding three times before samples were measured with XPS. All samples were placed on conductive carbon tabs and outgassed at 10^{-4} mbar for 20 minutes and then transferred to the ion-pumped analysis chamber. Pressure was kept below 5×10^{-7} Pa during data acquisition. Incident X-ray spot size was 100 μm and used an excitation of 100 W at 20 kV of the radiation source. The binding energies were aligned such that the C1s peak was fit to a peak center of 284.8 eV to account for charging effects. Prior to spectral shifting, C1s peaks were fit using a Shirley background and with 30% Gaussian-70% Lorentzian waveforms. An electron flood gun in addition to Ar^+ ion gun were used to minimize charging due to the nonconductive TiO_2 samples. Survey scans (0-1100 eV) were collected on each sample at multiple points before high resolution scans were collected. High resolutions scans were taken at least for 2 points. These two scans must reveal the same features in the S 2p for use in interpretation. Of the multiple scans taken, the spectra with the highest Ti 2p : C 1s area ratio were presented in the manuscript due to the likely highest fraction of sample to bare carbon tape. S 2p spectra were fit with 30% Gaussian-70% Lorentzian waveforms and $2p^{3/2}$ and $2p^{1/2}$ peaks had a fixed splitting of 1.2 eV based on 1.2 eV being the most common splitting value in the NIST spectral database.

Sample surface area and morphology was characterized using a Micromeritics 3-Flex pressure-based N_2 isotherm instrument. Nitrogen physisorption measurements used 12 mm borosilicate tubes containing (100±5) mg of powder samples. Samples were degassed in the Micromeritics SmartVacPrep unit with total pressure below 0.1 torr for 19 hours at 250 °C. Nitrogen adsorption isotherm measurements were taken in a bath of liquid nitrogen with saturation pressure of the bath measured at each point. The BET method was employed to determine sample surface areas.

Catalytic Characterization. Catalytic experiments were performed in a quartz U-Tube flow reactor with 1 cm bed diameter at ambient pressure. Each catalyst bed was made such that the bed height was (1±0.2) cm. In order to achieve this, for lightoff curves, undiluted catalyst beds of (80±1.5) mg were used and for kinetic experiments, in order to achieve low conversion (see below), samples were mixed with 200 mg calcined SiO_2 (Davisil >99%, calcined 900 °C for 5 hours) using a mortar and pestle before use. A bed of 200 mg of calcined SiO_2 was placed in 0.005 bar 2-propanol and balance Ar flow at 30 mL min^{-1} with no activity being observed until 215 °C to verify the lack of activity of the SiO_2 used. Mixing included grinding in a mortar and pestle for three cycles before color gradient was no longer visible between particles. Mixed powder was loaded and packed with

a glass rod into the U-Tube between immobilizing layers of acid-washed, calcined quartz. An additional 0.25-0.5 cm layer of quartz (mesh 180-425 μm) was added above the catalytic beds to preheat reaction gasses. The reactor was placed in the heated zone of a Micromeritics Eurotherm 2416 furnace with a thermocouple placed in the center of the bed. Gas flow mixtures were prepared with Brooks SLA5850 mass flow controllers and using diluted O_2 (5 vol. % in Ar, certified Airgas), and Ar (99.999% Airgas) in the gas phase. Alcohol reactants used were: 2-propanol (Sigma, 99.5%) and ethanol (Sigma, 99%) that were fed into reactant streams through a saturator at controlled temperature between 25 °C and 32 °C. Vapor pressures for 2-propanol and ethanol were determined using published Antoine coefficients.

Prior to each 2-propanol dehydration catalytic measurement, diluted catalyst beds were placed under a flow of 5 vol. % O_2 in Ar at a rate of 40 mL min^{-1} at 250 °C for 30 min and were then lowered to 80 °C under pure Ar flow at 40 mL min^{-1}. Similarly, prior to each ethanol dehydration catalytic measurement, diluted catalyst beds were placed under a flow of 5 vol. % O_2 in Ar at a rate of 40 mL min^{-1} at 350 °C for 30 min and were then lowered to 120 °C under pure Ar flow at 40 mL min^{-1}.

Concentrations of effluent gases in catalytic experiments were measured with FT-IR using a Thermo Fisher Nicolet is-50 FT-IR with a gas cell attachment with 200 mL of volume and a 2 m pathlength. The gas cell was affixed to the effluent of the U-tube reactor and FT-IR spectra of the gas phase was measured. After catalyst bed activation, U-tubes were bypassed, and feed mixtures were measured with effluent detection. During feed collection, Ar flow of 40 mL min^{-1} was maintained over the catalyst beds. All steady-state measurements were taken only after steady rates were collected after 5 gas cell volumes (1 L) of gas of a set composition had passed through the cell.

For 2-propanol experiments, calibration curves were developed for gas-phase reagents and products (isopropanol, propene, acetone, water and CO_2) within ranges of all reported conversions in this work, and no other products were detected for this reaction. Using the TQ analyst software package (from ThermoFisher), a partial least squares spectrum analysis method was generated to determine effluent gas composition. To generate the quantification method, 42 standard spectra with ranges from 0.0-0.5% of each component were measured. A mix of 50% single component

and 50% multiple component standards were included in the standard set. Using this method, product yield error ranges from 0.5% to 2%.

For ethanol experiments, individual peak heights were used to quantify component species in the effluent. For ethanol the O-H stretch at 3673 cm^{-1}, for acetaldehyde the C=O stretch at 1750 cm^{-1}, for water the O-H stretch from 4000 cm^{-1} to 3800 cm^{-1}, for ethylene the C=C-H bend at 950 cm^{-1} and for CO_2 the C=O asymmetric stretch at 2366 cm^{-1} were used. Estimates of response factors to determine concentration for each peak were determined by using spectra of known quantities of ethanol, water and CO_2 and were based on interpretation of analogous peaks in propene and acetone for ethylene and acetaldehyde. This method gives larger uncertainty leading to an estimated 10% error in product yield.

Alcohol conversion is calculated based on equation (4.1) and product yields are calculated based on equation (4.2):

$$Conversion\ (\%) = (1 - \frac{P_{Reactant(effluent)}}{P_{Reactant\ (feed)}}) * 100(\%) \quad (4.1)$$

$$Yield\ (\%) = \frac{P_{Product(effluent)}}{P_{Reactant\ (feed)}} * 100(\%) \quad (4.2)$$

Selectivity is calculated according to equation (3):

$$Selectivity_{Product\ A}(\%) = \frac{P_{Product\ A(effluent)}}{P_{Products\ total\ (effluent)}} * 100\ (\%) \qquad (4.3)$$

Kinetic values were taken from steady state points where conversion was below 5% and activity was steady (± <1% of measured yield) for 5 data points. These five data points are averaged to give the data plotted Arrhenius plots. Surface areas were taken from BET calculations on N_2 isotherms.

Propylamine desorption experiments. Propylamine desorption measurements were carried out in quartz U-Tube flow reactors with 1-cm bed diameter at ambient pressure. Samples were immobilized between acid-washed, calcined quartz layers similarly to temperature programmed dehydration measurements above. 200 mg of samples were loaded into the quartz U-tube for

analysis which were placed in a Micromeritics Eurotherm 2416 furnace with a thermocouple placed in the center of the bed. Beds were first placed under 50 mL min^{-1} Ar (99.999% Airgas) flow for 120 minutes at 300 °C to remove adsorbed components before cooling to 80 °C. 1-propylamine (Aldrich 99%) was added to the catalysts maintained at 80 °C through a saturator flowing 20 mL min^{-1} of argon at 25 °C for 30 minutes. After saturation with propylamine, the samples were purged with Ar at 80 °C for 1 hour at 40 mL min^{-1} followed with two hours at 20 mL min^{-1} to remove physisorbed propylamine. Under the same 20 mL min^{-1} flow, the sample beds were then heated at 10 °C min^{-1} until 740 °C. Products and propylamine were measured with a mass spectrometer residual gas analyzer (RGA, Hiden HPR 20) using the MASoft software package to track mass signals. Ar was tracked with m/z = 40, propene with m/z = 41, propylamine with m/z = 30 and finally ammonia with m/z = 17. All signals were normalized against Ar total pressure. Ammonia and propene are known to be produced from decomposition of propylamine on Brønsted acid sites[28] and as such relative areas of these products can give information on the concentration of Brønsted acid sites in the materials tested.

Results and Discussion

Results

Figure 2 displays light-off curves of catalyst beds containing equal masses of DMSO-treated TiO_2 (Figure 2a), H_2SO_4-treated TiO_2 (Figure 2b) and calcined TiO_2 for comparison (Figure 2c). As a convenient metric, comparison of the temperature at which 15% conversion is realized shows stark differences: 230 °C for calcined TiO_2, 150 °C for DMSO-treated TiO_2 and 145 °C for H_2SO_4 treated TiO_2. Therefore, within the measured temperature window, the propene yield is much higher with either sulfur-containing catalyst, with highest yields at high conversion for the DMSO-treated TiO_2 catalyst. Further, the product distribution is shifted from roughly equal production of acetone and propene in calcined TiO_2 (Figure 2c) to detection-limited complete selectivity to propene, the desired dehydration product, with DMSO-treated TiO_2 (Figure 2a). Carbon balance is not maintained in the case of calcined TiO_2 with an apparent accumulation of carbon on the TiO_2 surface being evident at temperatures above 240 °C due the absence of any other carbon-containing products detected in the gas phase. Given the 2% uncertainty in the reaction measurement through

FT-IR, the DMSO-treated TiO_2 shows a closed carbon balance with the eluted products. To test the catalyst stability, an additional catalyst bed of DMSO-treated TiO_2 was tested for 5 repeated light-off experiments with the propene yield results plotted in supplemental figure 1. Propene was the only product detected in these experiments. After a slight deactivation from the first thermal cycle, each of the four subsequent reaction cycles showed nearly identical light-off behavior, demonstrating the stability of this catalyst up to 250 °C when full conversion was reached.

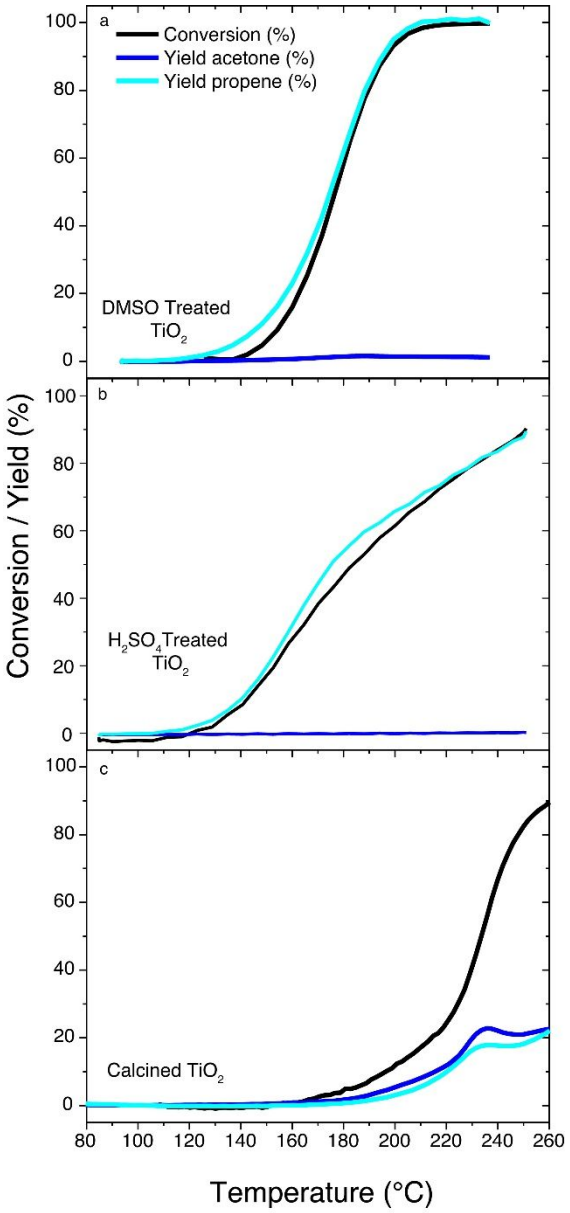

Figure 2. Light-off curves for (a) DMSO Treated TiO_2 and (b) H_2SO_4 Treated TiO_2 (c)calcined TiO_2. Conditions: 2-propanol (0.5 vol. %) + Argon, 50 mL min^{-1} total flow rate, 1°C min^{-1} ramp rate. Equal mass of catalyst in catalytic beds.

Figure 3 displays turnover frequencies calculated from low conversion (< 5%) kinetic measurements of isopropanol dehydration for calcined H_2SO_4-treated and DMSO-treated TiO_2. From these measurements it is clear that the activity normalized per surface area of DMSO-treated TiO_2 is roughly 50 times higher relative to the calcined TiO_2 control sample and higher than the H_2SO_4-treated TiO_2 sample by nearly an order of magnitude. From this data, apparent activation energies for 2-propanol dehydration of 122 kJ mol^{-1}, 126 kJ mol^{-1}, and 101 kJ mol^{-1} for calcined TiO_2, H_2SO_4-treated TiO_2, and DMSO-treated TiO_2 were calculated, respectively. The similar elevated activation energies for the calcined TiO_2 and the H_2SO_4-treated TiO_2 indicates similar reaction mechanisms for those surfaces which both contain Brønstead acid sites and a lower activation energy on the DMSO-treated TiO_2. Time-on-stream data presented in figure 3b shows the product yields and 2-propanol conversion over time for a 6-hour period where a DMSO-treated TiO_2 bed was kept at 190 °C in between the thermal cycles used to generate the plots in supplemental figure 1. There is stable performance for the whole length of this experiment. Selectivity is completely dominated by dehydration for the duration of the experiment, as well as for subsequent thermal cycles plotted in supplemental figure 1 (cycles 4 and 5) showing similar activity to those before this stability study (cycles 2 and 3). The data obtained from the stable performance demonstrated in figure 3b is plotted alongside reference selectivity values in supplemental figure 2 to highlight that DMSO-treated TiO_2 yields >99% dehydration selectivity at more than 100 °C lower than any previously reported TiO_2-based catalyst.

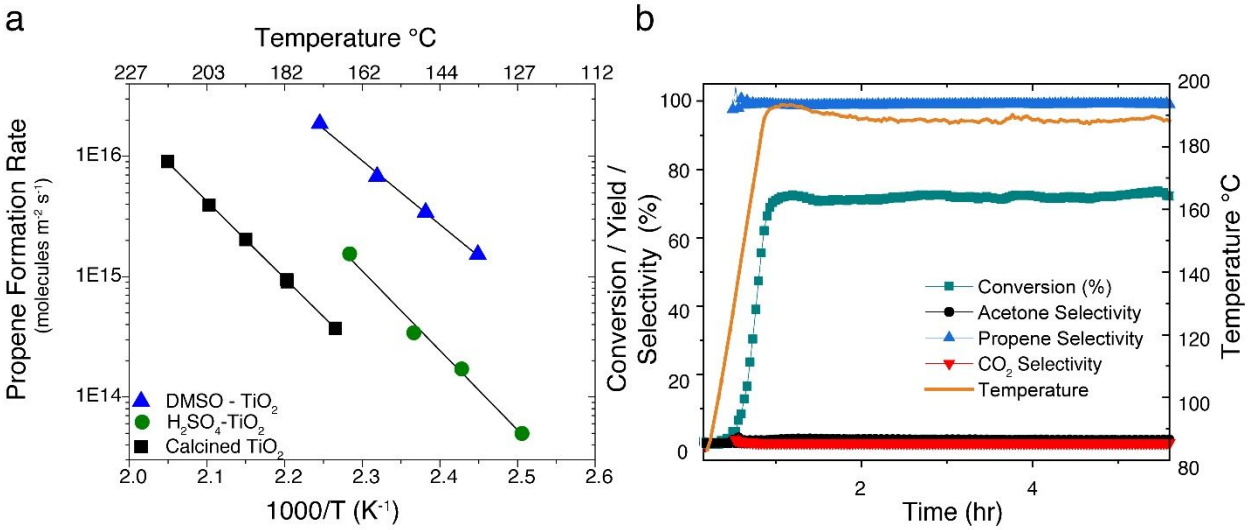

Figure 3 (a) Kinetic rates of 2-propanol dehydration on calcined commercial TiO_2 and DMSO-treated TiO_2. (b) Steady-state activity for DMSO-treated TiO_2, conditions: 2-propanol (0.5 vol%) + Argon, 3 °C min^{-1} ramp rate to 190 °C followed by dwell at this temperature. 50 mL min^{-1} total gas flow rate.

Figure 4 reports the S 2p XPS spectrum of several relevant materials: calcined TiO_2, DMSO-treated TiO_2 before and after catalysis, as well as H_2SO_4-treated TiO_2. As expected, calcined TiO_2 shows no appreciable peak whereas the DMSO-treated materials display sulfur species both before and after reaction. Previous interpretations of this contribution for sulfated TiO_2 as well as other reference compounds rule out the possibility of S(II) species like those which would be present in thiols or thioethers, which typically appear in the 160 to 165 eV region of the spectrum.[29] Pre-catalysis materials appear to contain oxidized sulfur species with S(IV) or S(VI) oxidation states[30] with an apparent equal area ratio of S(IV) and S(VI) species. In the spent catalyst, contrastingly, the S(IV) species appear to be strongly attenuated relative to the S(VI) species, accounting for only 22% of area present in the spectrum. In the spent catalyst, the S(VI) species appear to be further oxidized by nearly 1 eV such that the S(VI) species align with the sulfur species present in H_2SO_4-treated TiO_2. This shift is likely due to the pretreatment of catalyst beds at 250 °C under flowing 5% O_2. Elemental compositions determined by post reaction XPS of DMSO-TiO_2 indicate that after 15 hours on stream, sulfur content in the DMSO-treated TiO_2 is maintained at 74% of the

level of initial sulfur from deposition based on comparison of the ratio between sulfur $2p_{5/2}$ and titanium 2s peak heights.

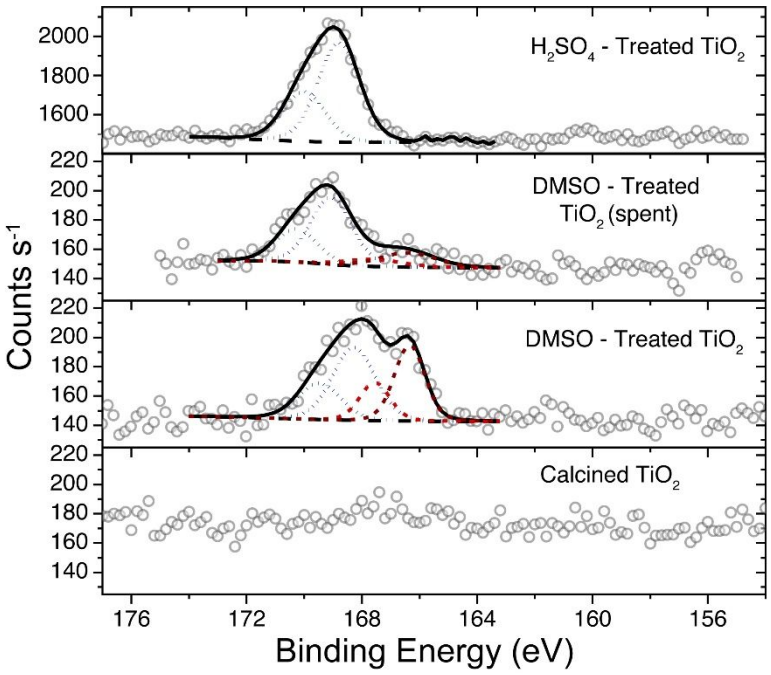

Figure 4: S 2p XPS of Calcined TiO_2, DMSO-treated TiO_2 as synthesized and spent catalyst (15 hours on stream), and H_2SO_4-treated TiO_2 as a reference.

Figure 5 contains temperature programmed desorption (TPD) experiments of 1-propylamine in fixed beds of 200 mg of DMSO-treated TiO_2, H_2SO_4-treated TiO_2 and calcined TiO_2. The integrated propylamine signal of 0.415 bar °C for calcined TiO_2 vs. 0.366 bar °C for DMSO-treated TiO_2 is roughly proportional to the BET area determined by nitrogen physisorption of 61 and 51 $m^2\ g^{-1}$, respectively, indicating that DMSO-treated TiO_2 contains roughly 85% of the available physical adsorption sites. When treating directly with H_2SO_4, nitrogen physisorption area is relatively unchanged at 57 $m^2\ g^{-1}$ while integrated propylamine area is 0.318 bar °C. Propene signal in the effluent of the TPD, which is indicative of Hoffman elimination of alkylamines at Brønsted acid sites,[28] is presented in Table 2 along with calculated Brønsted acid site concentrations. In comparing the Brønsted acid site concentrations, while there is an apparent decrease in Brønsted acid sites with DMSO treatment, there is only a 27% increase in Brønsted acid site concentration

on TiO_2 when impregnating with H_2SO_4 to an equal S:Ti atomic ratio as that of DMSO-treated TiO_2. Further, in repeating the TPD experiments after 15 hours on stream for alcohol dehydration catalysis (supplementary figure 5 and supplementary table 1), there is no apparent loss in Brønsted acid site concentration after reaction.

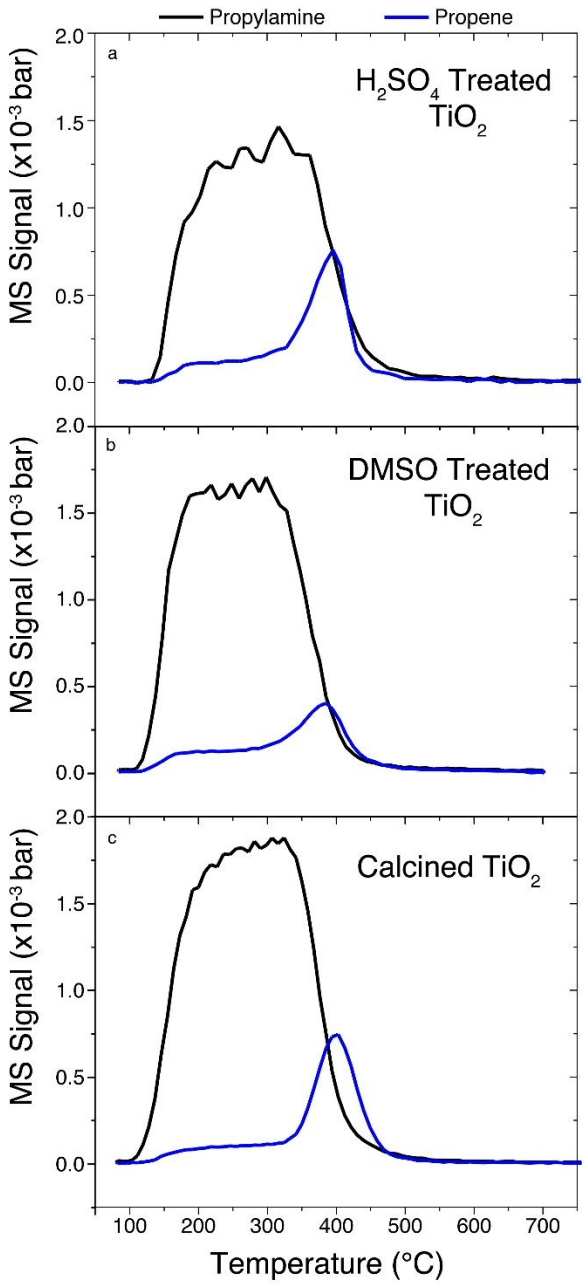

Figure 5 Propylamine TPD of (a) H_2SO_4-treated TiO_2 (b) DMSO-treated TiO_2 (c) calcined TiO_2 as a control. Conditions: 20 mL min^{-1} gas flow, 10 °C min^{-1} temperature ramp rate.

Table 2 Propylamine desorption peaks

Sample	Propylamine Desorption Area (bar °C)	Propene Desorption Area (bar °C)	Brønsted Acid Site Concentration (μmol g^{-1})
Calcined TiO_2	0.415	0.062	24.9
DMSO-treated TiO_2	0.366	0.036	14.6
H_2SO_4-treated TiO_2	0.318	0.079	31.6

Discussion

The mechanism of alcohol dehydration through the elimination reaction on metal oxides is well studied and proceeds through either the protonation of the hydroxyl group that leaves as water and resultant carbocation intermediate formation (E1), or through a concerted transition complex with simultaneous C-O bond breaking and β-elimination (E2). The catalytic data in figures 2 and 3 suggest that DMSO-treatment of TiO_2, in addition to increasing selectivity to the dehydration product by suppressing the dehydrogenation pathway to a carbonyl species (e.g. acetone), also accelerates the dehydration pathway, which must be due to stabilization of the transition state along the reaction coordinate.

Some potential ways by which either the E1 or E2 transition states could be stabilized on TiO_2 surfaces are: i) the introduction or increased availability of protons from Brønsted acid sites to promote an E1 mechanism; ii) the presence of a more reactive nucleophilic group to assist in the proton abstraction in a concerted E2 mechanism; iii) a Lewis acid site that are better capable of stabilizing a charged alkoxyl transition state; iv) the increased polarity at the surface near an acid site to stabilize the charged activated complex of either the E1 or E2 mechanism as hypothesized by Medlin and coworkers.[21]

Identification of the species present on the surface of the DMSO-treated TiO_2 can help identify most likely hypotheses for the observed effect. There are many potential species that could be present on calcined TiO_2 resulting from thermal decomposition of DMSO, especially in the presence of the solid acid TiO_2. Many researchers have quantified the decomposition products of

DMSO with some of the most commonly reported species being methanethiol, sulfur dioxide, carbon disulfide, and dimethylsulfane.[31–33] Based on the FTIR analysis of a heat-treated DMSO-TiO_2 sample presented in supplemental figure 3a, it is evident that any C-H containing compounds that are present on the surface of the TiO_2 after treatment are removed after 30 min under flowing 5% O_2 at 250 °C. Based on sulfur XPS before and after catalysis, it is also evident that the sulfur species present is in an oxidation state of S(IV) or S(VI), eliminating any thioether or thiol having S(II) species as the relevant species. Baltrusaitis and colleagues reported the mechanism for SO_2 adsorption onto TiO_2 nanoparticles[34] via adsorption into O vacancies and subsequent formation of sulfite (SO_3^{2-}) or sulfate (SO_4^{2-}) species depending on temperature and availability of oxygen, suggesting SO_2 as potential candidate of species in our synthesis conditions to react and deposit sulfur onto the TiO_2 surface.

In the pretreatment of the catalyst beds tested for this work, oxygen at 250 °C was used and would provide the conditions necessary to oxidize any SO_3^{2-} species into SO_4^{2-}. This further oxidation is clearly evident in the spent catalyst XPS presented in figure 4, which reveals that nearly all sulfur present is in the (VI) oxidation state, likely as sulfate based on the comparison with the H_2SO_4-treated TiO_2 sample. Further inspection of the FT-IR features in supplemental figure 3b, specifically in the region of 1100-1200 cm^{-1}, show a peak similar to that reported in literature of a sulfated TiO_2 sample,[35] further evidencing SO_4^{2-} presence in these samples as well as with the H_2SO_4-TiO_2 catalyst that we prepared.

Sulfate deposited onto metal oxide catalyst have long been reported for their high acidity and in some case superacidic character.[36,37] Literature reports also characterize limited gains in alcohol dehydration selectivity to olefins on these materials relative to their sulfur-free counterparts as well.[36] Sulfated TiO_2 has been characterized as an alcohol dehydration catalyst showing high activity with ionic species (H_2SO_4 and Na_2SO_4) that were used to treat samples of anatase and rutile TiO_2.[18,38,39] In many works, however, the structure with which sulfate binds to TiO_2 is clearly defined, with the addition of the strong Brønsted acid sites accounted for.[37,40] There is catalytic evidence that this sulfate-containing TiO_2 contributes to high activity and selectivity for 2-propanol dehydration in this work, with the propene yields of this study compared to literature values in supplemental figure 2.

Relative to DMSO-treated TiO_2, H_2SO_4-treated TiO_2 catalyst displays similar light-off temperature profiles to produce propene and does so while also maintaining high selectivity, yet tails off in propene yield above 170 °C (supplemental figure 4). This catalytic behavior indicates the presence of similar highly active sites compared to DMSO-treated TiO_2 that may become saturated in the case of H_2SO_4-treated TiO_2. Given the known poisoning of strongly acidic Lewis acid sites with SO_4^{2-} addition with ionic sulfating agents, it follows that the loss of these sites leads to the reduced conversion of H_2SO_4-TiO_2 above 170 °C .[18] This indicates that DMSO-treated TiO_2 contains Lewis acid sites to a higher degree than H_2SO_4-treated TiO_2. This discrepancy in specific sites is a result of the poisoning of Lewis acid sites with sulfate species in H_2SO_4-treated TiO_2 and from the creation of Lewis acid sites in the decomposition of DMSO in DMSO-treated TiO_2.

While spectroscopic evidence points to a sulfate-like species present in the DMSO-treated TiO_2 catalyst, it is also evident from propylamine TPD in figure 5 that these species do not possess similarly high density of Brønsted acid sites as calcined TiO_2 does. To provide clarity on the nature of the increased activity for the various sulfur-treated TiO_2 catalysts, we turned to ethanol dehydration, where the decreased stability of a potential primary carbocation forces the reaction to follow much more preferably an E2 elimination mechanism. Figure 6 shows the ethanol dehydration light-off behavior of DMSO-treated TiO_2, H_2SO_4-treated TiO_2 and calcined TiO_2. Both sulfur-containing catalysts exhibit an increase in activity and selectivity to dehydration with approximately 70% conversion (67% with H_2SO_4-treated TiO_2 and 74% for DMSO-treated TiO_2) and ~90% dehydration selectivity (94% H_2SO_4-treated TiO_2 and 90% for DMSO-treated TiO_2) at 325 °C compared with 23% conversion at 90% selectivity for the calcined TiO_2. The similarity in light-off behavior for ethanol dehydration for the DMSO-treated TiO_2 and H_2SO_4-treated TiO_2 suggests that sulfate species present on a TiO_2 surface are the dominant active sites for ethanol dehydration. With an intermediate stability of the secondary carbocation, 2-propanol may dehydrate by either an E1 or E2 type mechanism. The increased conversion of 2-propanol at elevated temperature over DMSO-treated TiO_2 relative to H_2SO_4-treated TiO_2 (Fig. 5b) therefore suggests that the DMSO-treated TiO_2 contains additional sites that are active for either stabilizing an additional E1 or E2-type pathway beyond the purely sulfate-based sites present in H_2SO_4-treated TiO_2. An additional Lewis acid site on DMSO could operate through either type of mechanism. Relating to potential mechanisms of catalysis mentioned earlier, the additional Lewis acid sites could operate by acting as a stronger nucleophile than is present on H_2SO_4-treated TiO_2,

by better stabilizing the charged alkoxyl transition state in either ethanol or isopropanol dehydration, or by increasing the surface polarity which could in turn stabilize either a concerted or a sequential transition state.

The comparison of ethanol vs isopropanol dehydration therefore shows how the DMSO treatment produces active species that can operate through multiple mechanisms for alcohol dehydration, leading to overall higher conversion and selectivity relative to H_2SO_4-treated TiO_2. Combined with the known poisoning of some strongly acidic Lewis acid sites with SO_4^{2-} addition from ionic sulfating agents, it is highly likely that DMSO treatment leaves these same Lewis acid sites intact in light of the primary vs secondary alcohol catalytic dehydrogenation results.

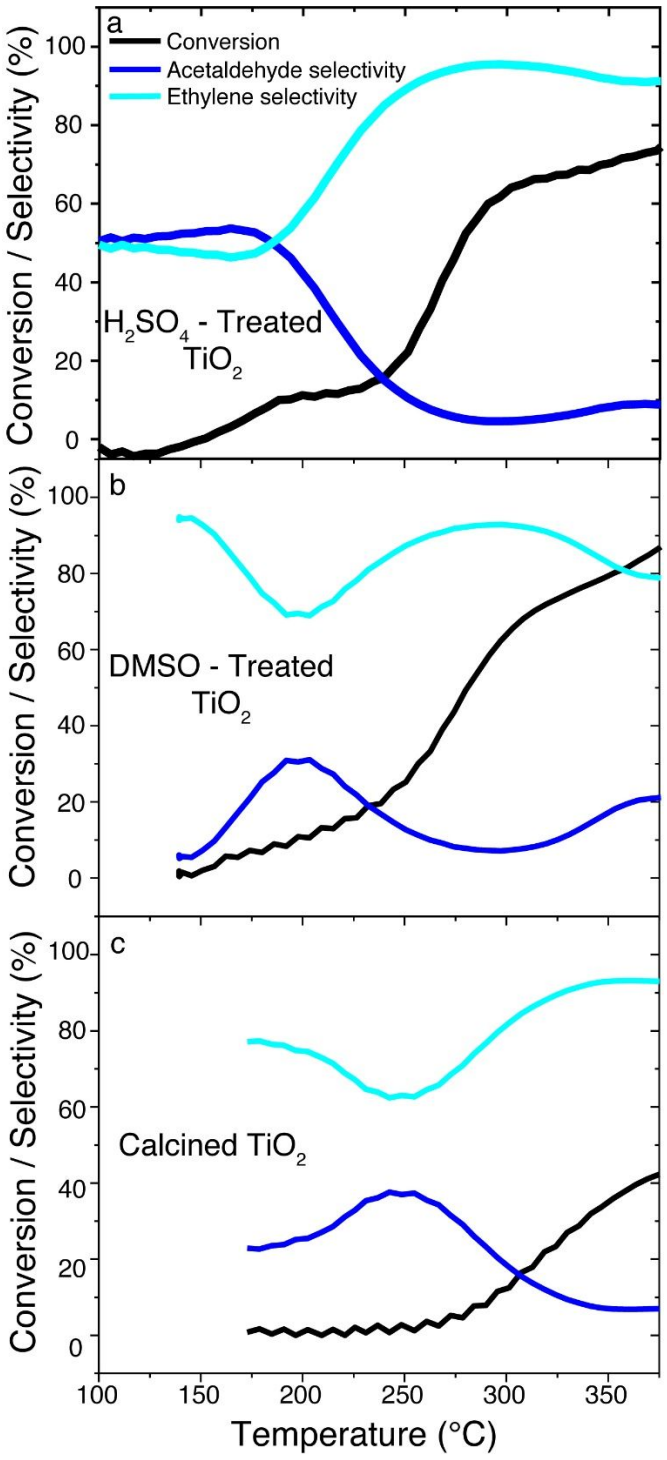

Figure 6 Ethanol dehydration lightoff curves (a) H_2SO_4 treated TiO_2, (b) DMSO-Treated TiO_2, and (c) Calcined TiO_2. Conditions: Ethanol (0.5 vol%) + Argon 40 mL/min, 1°C min^{-1} ramp rate. Equal mass of catalyst in beds.

The exact nature of the species present on the highly active and selective DMSO-TiO_2 catalyst remains unclear beyond the evidence of sulfate units. Lewis acid sites present on TiO_2 that are not poisoned with DMSO treatment remain the most likely candidate species and future studies can help identify these species as the reason for TiO_2 improvement upon DMSO treatment in dehydration catalysis of both primary and secondary alcohols.

Conclusions

In this work we detail the synthesis of a highly active alcohol dehydration catalyst from the treatment of commercially available TiO_2 powder with dimethyl sulfoxide (DMSO). This catalyst has nearly two orders of magnitude improved rates in 2-propanol dehydration with nearly complete selectivity to the dehydration product propylene. XPS and FT-IR demonstrate the presence of sulfate-containing species in the DMSO-treated TiO_2. Based on control tests with H_2SO_4-treated TiO_2, there is a clear distinction between the action of H_2SO_4-created sulfate species and those deposited from DMSO. This difference leads to DMSO-treated TiO_2 performing with equal or higher activity and selectivity for primary and secondary alcohol dehydration than even H_2SO_4-treated TiO_2. While the exact structure of the active site is not fully clear, the apparent decrease in the poisoning of highly active Lewis acid sites from DMSO sulfation relative to H_2SO_4 sulfation demonstrates that sulfating metal oxides with alternative sulfating agents can be beneficial to catalyst performance.

Acknowledgements

We gratefully acknowledge the contributions of Juliet Jamtgaard for assistance with XPS characterization and An-Chih Yang for help in Temperature Programmed Desorption. A.R.R. was supported by the National Science Foundation Graduate Research Fellowship Program award number DGE-1656518. M.C. acknowledges support from a Sloan Fellowship in Chemistry. Part of this work was performed at the Stanford Nano Shared Facilities (SNSF), supported by the National Science Foundation under award ECCS-1542152.

References

(1) Amarasekara, A. S.; Williams, L. T. D.; Ebede, C. C. Mechanism of the Dehydration of D-Fructose to 5-Hydroxymethylfurfural in Dimethyl Sulfoxide at 150 °C: An NMR Study. *Carbohydr. Res.* **2008**, *343* (18), 3021–3024.

(2) Kllç, E.; Yllmaz, S. Fructose Dehydration to 5-Hydroxymethylfurfural over Sulfated TiO2-SiO2, Ti-SBA-15, ZrO2, SiO2, and Activated Carbon Catalysts. *Ind. Eng. Chem. Res.* **2015**, *54* (19), 5220–5225.

(3) Alonso, D. M.; Bond, J. Q.; Dumesic, J. A. Catalytic Conversion of Biomass to Biofuels. *Green Chem.* **2010**, *12* (9), 1493–1513.

(4) Lehr, V.; Sarlea, M.; Ott, L.; Vogel, H. Catalytic Dehydration of Biomass-Derived Polyols in Sub- and Supercritical Water. *Catal. Today* **2007**, *121* (1–2), 121–129.

(5) Tendam, J.; Hanefeld, U. Renewable Chemicals: Dehydroxylation of Glycerol and Polyols. *ChemSusChem* **2011**, *4* (8), 1017–1034.

(6) Nash, C. P.; Ramanathan, A.; Ruddy, D. A.; Behl, M.; Gjersing, E.; Griffin, M.; Zhu, H.; Subramaniam, B.; Schaidle, J. A.; Hensley, J. E. Mixed Alcohol Dehydration over Brønsted and Lewis Acidic Catalysts. *Appl. Catal. A Gen.* **2016**, *510*, 110–124.

(7) Mohsenzadeh, A.; Zamani, A.; Taherzadeh, M. J. Bioethylene Production from Ethanol: A Review and Techno-Economical Evaluation. *ChemBioEng Rev.* **2017**, *4* (2), 75–91.

(8) Bedia, J.; Ruiz-Rosas, R.; Rodríguez-Mirasol, J.; Cordero, T. A Kinetic Study of 2-Propanol Dehydration on Carbon Acid Catalysts. *J. Catal.* **2010**, *271* (1), 33–42.

(9) Fan, D.; Dai, D. J.; Wu, H. S. Ethylene Formation by Catalytic Dehydration of Ethanol with Industrial Considerations. *Materials (Basel).* **2013**, *6* (1), 101–115.

(10) Collins, D. J.; Watters, J. C.; Davis, B. H. Catalytic Conversion of Alcohols. 13. Alkene Selectivity with Ti02 Catalysts. *Ind. Eng. Chem. Prod. Res. Dev.* **1979**, *18* (3), 202–205.

(11) Ai, M.; Suzuki, S. A Study of Catalytic Partial Oxidation of Hydrocarbons. XIII. The Effect of Bi2O3 Content in MoO4-Bi2O3-P2O5 Catalysts on the Dehydration of Isopropyl Alcohol. *Bull. Chem. Soc. Jpn.* **1973**, *46*, 321–322.

(12) Ai, M. Catalytic Activity for the Oxidation of Methanol and the Acid-Base Properties of Metal Oxides. *J. Catal.* **1978**, *54* (3), 426–435.

(13) Ai, M.; Suzuki, S. Effects of Acid-Base on Oxidation Properties Activity of MoO3-Bi2O3-P2O5 Catalysts and Selectivity. *Bull Japan Pet Inst* **1974**, *2*, 118–123.

(14) Kulkarni, D.; Wachs, I. E. Isopropanol Oxidation by Pure Metal Oxide Catalysts: Number of Active Surface Sites and Turnover Frequencies. *Appl. Catal. A Gen.* **2002**, *237* (1–2), 121–137.

(15) Haffad, D.; Chambellan, A.; Lavalley, J. C. Propan-2-Ol Transformation on Simple Metal Oxides TiO2, ZrO2 and CeO2. *J. Mol. Catal. A Chem.* **2001**, *168* (1–2), 153–164.

(16) Rekoske, J. E.; Barteau, M. A. Kinetics and Selectivity of 2-Propanol Conversion on Oxidized Anatase TiO2. *J. Catal.* **1997**, *165* (1), 57–72.

(17) Puigdollers, A. R.; Schlexer, P.; Tosoni, S.; Pacchioni, G. Increasing Oxide Reducibility : The Role of Metal / Oxide Interfaces in the Formation of Oxygen Vacancies. *ACS Catal.* **2017**, *7*, 6493–6513.

(18) Waqif, M.; Bachelier, J.; Saur, O.; Lavalley, J. C. Acidic Properties and Stability of Sulfate-Promoted Metal Oxides. *J. Mol. Catal.* **1992**, *72* (1), 127–138.

(19) Kim, Y. K.; Kay, B. D.; White, J. M.; Dohnálek, Z. Alcohol Chemistry on Rutile TiO2(110): The Influence of Alkyl Substituents on Reactivity and Selectivity. *J. Phys. Chem. C* **2007**, *111* (49), 18326–18342.

(20) Ellis, L. D.; Ballesteros-Soberanas, J.; Schwartz, D. K.; Medlin, J. W. Effects of Metal Oxide Surface Doping with Phosphonic Acid Monolayers on Alcohol Dehydration Activity and Selectivity. *Appl. Catal. A Gen.* **2019**, *571* (December 2018), 102–106.

(21) Ballesteros-Soberanas, J.; Ellis, L. D.; Will Medlin, J. Effects of Phosphonic Acid Monolayers on the Dehydration Mechanism of Aliphatic Alcohols on TiO2. *ACS Catal.* **2019**, *9* (9), 7808–7816.

(22) Tresatayawed, A.; Glinrun, P.; Jongsomjit, B. Ethanol Dehydration over WO3/TiO2 Catalysts Using Titania Derived from Sol-Gel and Solvothermal Methods. *Int. J. Chem.*

Eng. **2019**, *2019*.

(23) Cunningham, J.; Hodnett, B. K.; Ilyas, M.; Tobin, J.; Leahy, E. L.; Fierro, J. L. G. Dehydrogenation versus Dehydration of Aliphatic Alcohols on Metal Oxides. *Faraday Discuss. Chem. Soc.* **1981**, *72* (C), 283–302.

(24) Ellis, L. D.; Trottier, R. M.; Musgrave, C. B.; Schwartz, D. K.; Medlin, J. W. Controlling the Surface Reactivity of Titania via Electronic Tuning of Self-Assembled Monolayers. *ACS Catal.* **2017**, *7* (12), 8351–8357.

(25) Dahl, S.; Logadottir, A.; Egeberg, R. C.; Larsen, J. H.; Chorkendorff, I.; Törnqvist, E.; NØrskov, J. K. Role of Steps in N2 Activation on Ru(0001). *Phys. Rev. Lett.* **1999**, *83* (9), 1814–1817.

(26) Torres Galvis, H. M.; Koeken, A. C. J.; Bitter, J. H.; Davidian, T.; Ruitenbeek, M.; Dugulan, A. I.; De Jong, K. P. Effects of Sodium and Sulfur on Catalytic Performance of Supported Iron Catalysts for the Fischer-Tropsch Synthesis of Lower Olefins. *J. Catal.* **2013**, *303*, 22–30.

(27) Krishnakumar, B.; Swaminathan, M. A Recyclable and Highly Effective Sulfated TiO2-P25 for the Synthesis of Quinoxaline and Dipyridophenazine Derivatives at Room Temperature. *J. Organomet. Chem.* **2010**, *695* (24), 2572–2577.

(28) Kresnawahjuesa, O.; Gorte, R. J.; Oliveira, D. De; Lau, L. Y. A Simple , Inexpensive , and Reliable Method for Measuring Brùnsted- Acid Site Densities in Solid Acids. *Catal. Letters* **2002**, *82* (3), 155–160.

(29) Calloni, A.; Brambilla, A.; Berti, G.; Bussetti, G.; Canesi, E. V.; Binda, M.; Petrozza, A.; Finazzi, M.; Ciccacci, F.; Duò, L. X-Ray Photoemission Spectroscopy Investigation of the Interaction between 4-Mercaptopyridine and the Anatase TiO2 Surface. *Langmuir* **2013**, *29* (26), 8302–8310.

(30) Topalian, Z.; Niklasson, G. A.; Granqvist, C. G.; Österlund, L. Spectroscopic Study of the Photofixation of SO 2 on Anatase TiO 2 Thin Films and Their Oleophobic Properties. *ACS Appl. Mater. Interfaces* **2012**, *4* (2), 672–679.

(31) Hergenrother, L. Decomposition of Dimethyl Sulfoxide Aided by Ethylene Glycol,

Acetamide, and Related Compounds. *J. Org. Chem.* **1964**, *4019* (5), 1962–1963.

(32) Thyrion, F. C.; Debecker, G. Thermolysis of Dimethyl Sulfoxide. *Int. J. Chem. Kinet.* **1973**, *5* (4), 583–592.

(33) Head, D. L.; Mccarty, C. G. The Thermal Decomposition of DMSO. *Tetrahedron Lett.* **1973**, 1405–1408.

(34) Baltrusaitis, J.; Jayaweera, P. M.; Grassian, V. H. Sulfur Dioxide Adsorption on TiO2 Nanoparticles: Influence of Particle Size, Coadsorbates, Sample Pretreatment, and Light on Surface Speciation and Surface Coverage. *J. Phys. Chem. C* **2011**, *115* (2), 492–500.

(35) Allodi, V.; Brutti, S.; Giarola, M.; Sgambetterra, M.; Navarra, M. A.; Panero, S.; Mariotto, G. Structural and Spectroscopic Characterization of A Nanosized Sulfated TiO2 Filler and of Nanocomposite Nafion Membranes. *Polymers (Basel).* **2016**, *8* (3).

(36) Corma, A. Inorganic Solid Acids and Their Use in Acid-Catalyzed Hydrocarbon Reactions. *Chem. Rev.* **1995**, *95* (3), 559–614.

(37) Oi, L. E.; Choo, M. Y.; Lee, H. V.; Ong, H. C.; Hamid, S. B. A.; Juan, J. C. Recent Advances of Titanium Dioxide (TiO2) for Green Organic Synthesis. *RSC Adv.* **2016**, *6* (110), 108741–108754.

(38) Ma, Z.; Yue, Y.; Deng, X.; Gao, Z. Nanosized Anatase TiO2 as Precursor for Preparation of Sulfated Titania Catalysts. *J. Mol. Catal. A Chem.* **2002**, *178* (1–2), 97–104.

(39) Das, D.; Mishra, H. K.; Parida, K. M.; Dalai, A. K. Preparation, Physico-Chemical Characterization and Catalytic Activity of Sulphated ZrO2-TiO2 Mixed Oxides. *J. Mol. Catal. A Chem.* **2002**, *189* (2), 271–282.

(40) Noda, K.; Gonc, N. S.; Almeida, R. M. De; Meneghetti, S. M. P.; Meneghetti, M. R. Transesterification Reaction of Vegetable Oils , Using Superacid Sulfated TiO 2 – Base Catalysts. *Appl. Catal. A Gen.* **2008**, *347* (3), 100–105.